Tutorial for Space-Time ICI Parallel Cancellation Techniques for OFDM Systems

Hen-Geul Yeh, California State University, Long Beach, USA*

ABSTRACT

Orthogonal frequency division multiplexing (OFDM) expects the subcarriers to be orthogonal. However, the factors, such as residual carrier frequency, offset time variations due to Doppler shift or phase noise leads to a loss in the orthogonality between subcarriers and results in inter-carrier interference (ICI). Further developing the parallel cancellation (PC) scheme to mitigate the ICI of OFDM systems, the authors expand this OFDM symbol-based PC scheme into a space-time (ST) coded system. This simple space-time parallel cancellation (STPC) scheme is a technique that combines the useful properties of ST and PC schemes together. Computer simulations indicate that OFDM systems using the STPC scheme outperform the regular PC and ST systems in slow and fast frequency selective fading channels, specifically at a high signal-noise ratio (SNR). Furthermore, the error floor of the STPC-OFDM system is significantly lower than that of the regular ST systems without increasing computational load.

KEYWORDS

Inter-Carrier Interference, Orthogonal Frequency Division Multiplexing, Parallel Cancellation, Space-Time

INTRODUCTION

Orthogonal frequency division multiplexing (OFDM) communication systems have received substantial consideration as a bandwidth efficient modulation and multiplexing technical scheme for high data rate wireless applications, specifically for the 3rd, 4th, and 5th generations (3G, 4G, 5G) of cellular technology. Many applications, such as internet of things (IOT), unmanned aerial vehicle (UAV), wearable devices, and health monitoring devices are identified in the daily operation and usages. However, the factors such as carrier frequency offset, time variations due to Doppler shift or phase noise led to a loss in the orthogonality between subcarriers and results in inter-carrier interference (ICI) which degrades the bit error rate (BER) performance of OFDM systems significantly. Many ICI mitigation schemes such as ICI self-cancellation (SC), frequency-domain equalization, and the time domain windowing scheme have been proposed (Alamouti, 1988; Yeh & Wang, 2004; Yu et al., 2007; Seyedi & Saulnier, 2005; Yeh et al., 2007). The well-known SC method in (Alamouti, 1988) applies the repetitive transmission in a per-subcarrier basis, while the parallel cancellation (PC) (Yeh & Wang, 2004; Yeh & Zhou, 2022) apply the repetitive transmission in a per-OFDM symbol basis.

*Corresponding Author

Further developing the idea of the PC scheme to mitigate the ICI of OFDM systems, we expand this PC scheme into a space-time (ST) coded system (Alamouti, 1988; Li & Xia, 2008; Yusof & Zamani, 2008) and form a simple STPC-OFDM system. Since the ST scheme is robust to block size, the STPC scheme is also robust to block size. Additionally, the PC scheme provides a much higher signal-to-ICI ratio (SICIR) than does the regular OFDM system when Doppler shift or residual carrier frequency offset (CFO) exists. Hence the PC scheme lowers error floor for OFDM systems in frequency selective fading channels with Doppler frequency. This characteristic is extended to the STPC-OFDM system and improves the BER significantly. We focus on the architecture and BER performance comparison of the PC-, ST- and STPC-OFDM systems via simulations in frequency selective fading channels. Although our primary focus is the performance of STPC with frequency offset, STPC also performs well when ICI is caused by other factors, such as phase noise, timing error, and time varying channels. Since the scheme is very simple, they can be applied to mitigate ICI alone, or combined with techniques, such as channel coding schemes to further improve diversity gain and coding gain in multiple input single output (MISO) and multiple input multiple output (MIMO) systems with industrial and commercial applications, such as robots, and sensors, manufacture, and smart factory, etc. There are other software defined radio transceivers and networks (Chang et al., 2012, 2013; Yeh & Ingerson, 2010; Nasir et al., 2016; Wen et al., 2013; Ma, 2017; Kumar & Rao, 2018) which can be combined with MIMO to further enhance systems performance and lower cost. Moreover, (Yeh & Zhou, 2022) shows that a higher modulation scheme compensates the bandwidth efficiency in the STPC-OFDM and STCC-OFDM schemes.

This tutorial paper is organized as follows. The OFDM system model is discussed with the weighting function of data in Section II. Section III briefs the PC scheme. Section IV shows the ST-OFDM system. Section V presents the STPC scheme. Sequential implementation of the STPC-OFDM system is discussed in Section VI. Section VII provides simulation results. Conclusions are presented in Section VIII.

THE REGULAR OFDM SYSTEM

For convenience and without loss of generality, the additive white Gaussian noise (AWGN) and the phase noise are omitted in the following discussion, except AWGN used in simulation. Figure 1 shows a simplified regular OFDM system. The baseband transmitted signal x_k at the output of the IFFT is

$$x_k = \sum_{n=0}^{N-1} d_n e^{j\frac{2\pi}{N}kn} \quad k = 0,1,2,...,N-1 \tag{1}$$

where d_n is the data symbol, and $e^{j\frac{2\pi}{N}kn}$, $k = 0,1,...,N-1$ represents the index of N subcarriers. After adding the cyclic prefix (CP), the signal $x^g = [x_{N-G}....x_{N-1}x_0....x_{N-1}]^T$ is transmitted. At the receiver (Rx), the received signal is the convolution of $\boldsymbol{x}^g$ and the channel impulse response $\boldsymbol{h}$. This signal is mixed with a local oscillator signal, which is ε above the correct carrier frequency. At the baseband, CP removal (CPR) and serial to parallel (S/P) are performed first. After FFT, the P/S conversion is performed, and the recovered symbol is obtained as depicted in Figure 1(b). The baseband recovered signal after FFT is

$$\hat{d}_m = \frac{1}{N}\sum_{k=0}^{N-1} r_k e^{-j\frac{2\pi mk}{N}} = \frac{1}{N}\sum_{n=0}^{N-1}\sum_{k=0}^{N-1} H_n d_n e^{j\frac{2\pi(n+\varepsilon)k}{N}} e^{-j\frac{2\pi mk}{N}} =$$
$$= d_m H_m u_0 + \sum_{n=0,n\neq m}^{N-1} d_n H_n u_{n-m} \quad m = 0,...,N-1 \tag{2}$$

where

$$u_{n-m} = \left. \frac{e^{j\pi\frac{N-1}{N}(n-m+\varepsilon)} \sin\left[\pi\left(n-m+\varepsilon\right)\right]}{N \cdot \sin\left[\left(\frac{\pi}{N}\right) \cdot \left(n-m+\varepsilon\right)\right]} \right|_{(n-m)\bmod N} . \tag{3}$$

In (2), r_k is the received signal to the FFT; k is the sampling index; $e^{j\frac{2\pi}{N}k\varepsilon}, k = 0,1,...,N-1$ represents the frequency offset of the received signal at the sampling instants; ε is the frequency offset normalized to the subcarrier frequency spacing; m is the receiver subcarrier index; H_n is the n-th element of the N-point FFT of the channel impulse response $\boldsymbol{h} = [h_0 ... h_k ... h_L\ 0\ ...0]^T$ with N-L-1 padding zeros; and u_{n-m} is the weighting factor on the data symbol. Note that the signal is transmitted through a fading channel of order L, i.e., the channel impulse response $h_k = 0$ for $k > L$. To avoid inter-symbol interference (ISI), the guard interval must be chosen to satisfy $G \geq L$. A well-known property of the FFT is that the cyclic convolution in the time domain results in multiplication in the frequency domain. Therefore, OFDM with a cyclic prefix transforms a frequency selective fading channel into N flat fading channels as shown in (2). For simplicity, slow fading channels with a constant mean of H_n are assumed. The averaged weighting function u_{n-m} is plotted in Figure 2 as a function of the normalized frequency of N=8. At ε =0, all weighting factors for d_n, n=1 to 7, are zeros except that the real part of u_0 equals one. This means it holds *orthogonality* and has no crosstalk among subcarriers. When ε >0, the curve of the weight function of Figure 2 shifts to the left and causes a loss of the subcarriers' *orthogonality*. Weights on data symbols are non-zero valued and ICI occurs. To mitigate ICI, a PC scheme is developed. The basic idea is to have a 2nd path that provides the curve of weighting factors with a right shift when ε >0. By combining these two-path data at the receiver, we show that the ICI will be significantly reduced due to the opposite polarity of the weighting function on all data except the desired data as shown in next section.

Figure 1. Architecture of a simplified OFDM baseband transceiver

(a) OFDM transmitter.

(b) OFDM receiver.
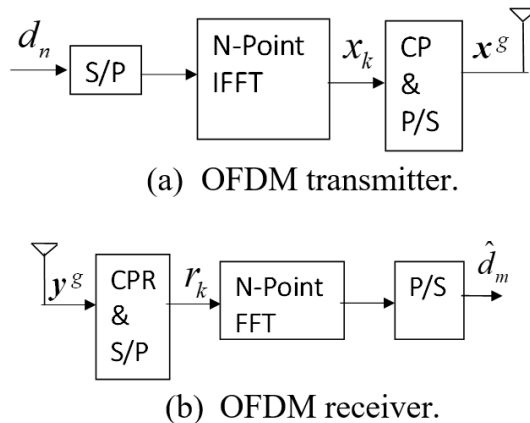
Figure 2. Weighting function of data symbols in the regular branch
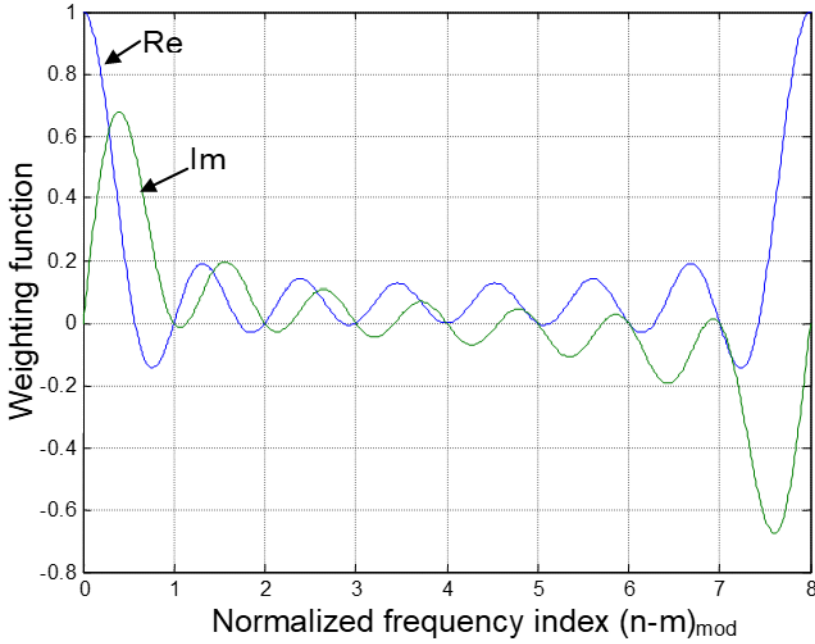
The PC Scheme

The PC scheme has a regular and a 2nd path operation. At the transmitter, the 2nd lower branch requires an FFT as defined in (4):

$$x_k^{'} = \sum_{n=0}^{N-1} d_n e^{-j\frac{2\pi}{N}kn} \quad k = 0,1,2,...,N-1.$$

(4)

where d_n is the data symbol. After adding the CP, the signal is transmitted. In order to transmit the first signal x_k and the second signal $x_k^{'}$ without interferences, time division multiplexing (TDM) is employed as depicted in Figure 3.

At the Rx, it employs a single Rx antenna with a de-multiplexer (DeMUX) to separate the first and the second branch received signals r_k and $r_k^{'}$ followed by a CP remover (CPR). Assuming that a TDM works well at the Tx, the Rx operates a N-point (N-Pt) FFT (the upper branch), and then does a IFFT operation (the lower branch), respectively. Assuming the synchronization has performed at the Rx, the demodulated signal of the 2nd branch after IFFT is

$$\hat{d}_m^{'} = \frac{1}{N} \sum_{k=0}^{N-1} r_k^{'} e^{j\frac{2\pi mk}{N}} = \frac{1}{N} \sum_{n=0}^{N-1} \sum_{k=0}^{N-1} H_n^{'} d_n e^{j\frac{2\pi(-n+\varepsilon)k}{N}} e^{j\frac{2\pi mk}{N}}$$

$$= d_m H_m^{'} v_0 + \sum_{n=0,n\neq m}^{N-1} d_n H_n^{'} v_{n-m} \quad m = 0,...,N-1$$

(5)

where

Figure 3. The architecture of a simplified baseband PC-OFDM transceiver
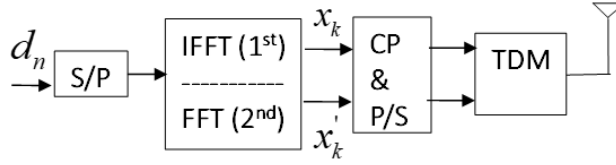
a. The transmitter

b. The receiver

$$
v_{n-m} = \left| \frac{e^{j\pi\frac{N-1}{N}(m-n+\varepsilon)} \sin\left[\pi\left(m-n+\varepsilon\right)\right]}{N \cdot \sin\left[\left|\frac{\pi}{N}\right| \cdot \left(m-n+\varepsilon\right)\right]} \right|_{(n-m)\bmod N} .
\tag{6}
$$

The same ε is applied in (5) – (6) since the local oscillator of the transceiver of the 2nd branch is the same as that of the 1st branch. Again, m is the receiver subcarrier index, H'_n is the n-th element of the N-point IFFT of the channel impulse response $\boldsymbol{h}' = [h'_0...h'_k...h'_L\ 0\ ...0]^T$ with N-L-1 padding zeros, and v_{n-m} is the weighting factor on the data symbol. Note that v_{n-m} is similar to u_{n-m} but the sign of $(n\text{-}m)$ is swapped. When $\varepsilon > 0$, a shift to the right operation on the weighting curve will occur. Figure 4 depicts the weighting function v_{n-m} of $N=8$ at $\varepsilon = 0$.

Since the PC scheme is a per-OFDM symbol basis technique, both 1st and 2nd branches can be combined coherently. In AWGN channels, $H_n = H'_n = I$ and the final detected symbol is obtained in (7).

$$
\hat{d}''_m = \hat{d}_m + \hat{d}'_m = d_m\left(u_0 + v_0\right) + \sum_{\substack{n=0 \\ n\neq m}}^{N-1} d_n\left(u_{n-m} + v_{n-m}\right) m = 0,...,N-1
\tag{7}
$$

The first term in (7) is the desired signal component and the 2nd term represents the ICI term. In this scheme, the imaginary component of weighting functions in Figure 4 is the negative version of that of Figure 2. By adding weights together, we show that the weights become a real valued function at $\varepsilon = 0$. Figure 5 depicts the combined weights with $N=16$ and $\varepsilon = 0.2$.

The SICIR in AWGN is defined in (8) and plotted in Figure 6 which compares SICIR among three OFDM systems: regular, SC, and PC schemes in the AWGN channel.

Figure 4. Weighting function of data in the 2ⁿᵈ branch with N=8
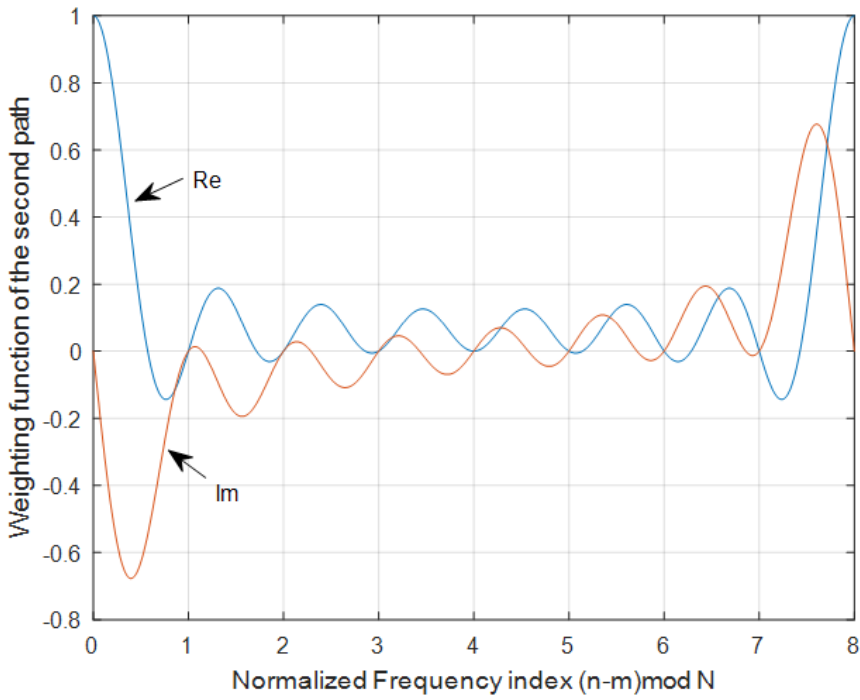
Figure 5. Magnitude of weighting factors of the regular and PC systems
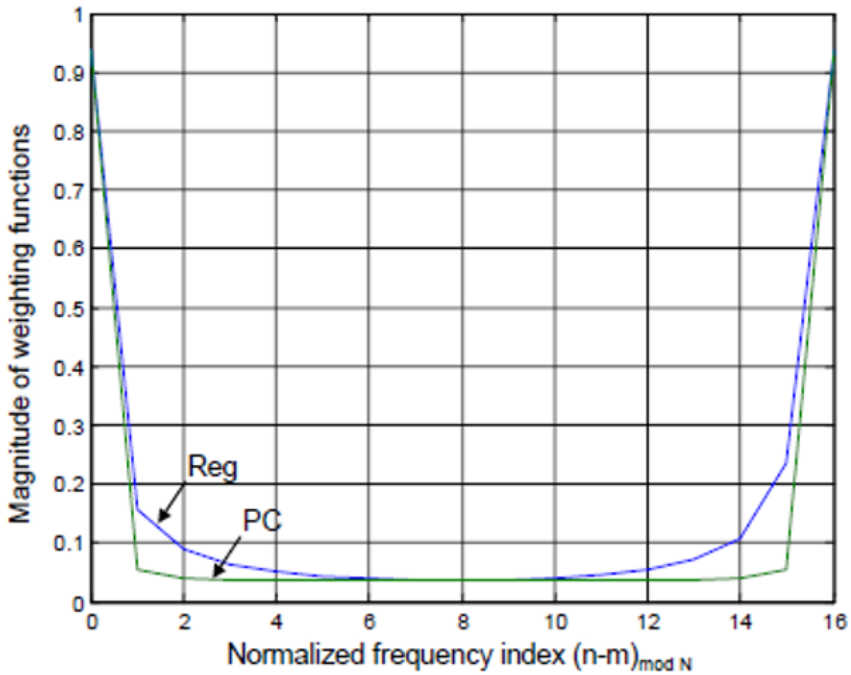
$$SICIR = 10 \log \frac{\left| u_0 + v_0 \right|^2}{\sum_{n=1}^{N} \left| u_n + v_n \right|^2} \, dB \qquad (8)$$

The SICIR of regular and SC systems is independent of N. On the other hand, the SICIR of the PC scheme is higher at larger N. Moreover, the SICIR of the PC scheme is notably larger than that of the SC scheme in a small ε range from 0 to 0.17 at N=8192, while the SC scheme is better than the PC scheme for ε larger than 0.17. In this paper, we consider the frequency synchronization to have already been done via preamble sequences; only motion-induced Doppler shift or small residual CFO may cause ICI. Consequently, PC is selected for integrating with ST coding and forms STPC scheme to mitigate ICI in the following sections.

$$\boldsymbol{d}_1 = [d_0 d_1 ... d_{N-2} d_{N-1}]^T, \qquad (9a)$$
$$\boldsymbol{d}_2 = [d_N d_{N+1} ... d_{2N-2} d_{2N-1}]^T. \qquad (9b)$$

The ST-OFDM Scheme

The ST-OFDM (Alamouti, 1988) applies the ST transmitter diversity technique in a per-OFDM symbol basis. In a [2x1] system, two length N consecutive blocks are formed as input data vectors at the transmitter as follows.

Figure 6. SICIR comparison among regular OFDM, PC, and SC schemes
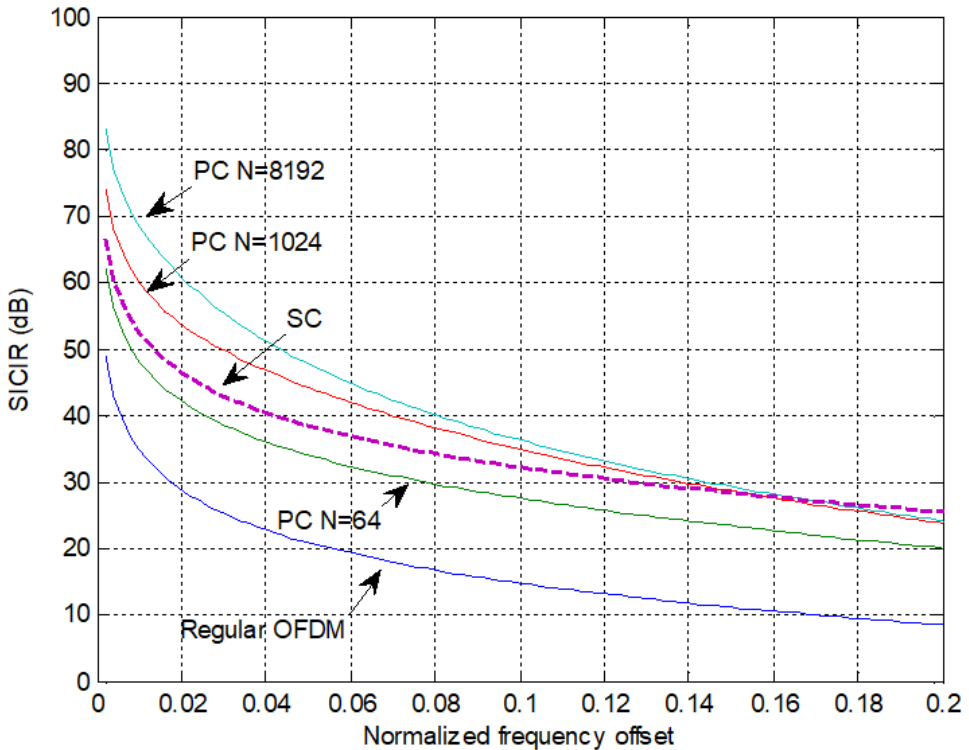
The baseband operations are performed at the Tx side. At time t, and $t+T$, $\boldsymbol{d}_1$ and $\boldsymbol{d}_2$, and $-\boldsymbol{d}_2^*$ and $\boldsymbol{d}_1^*$, are sent to two parallel branches for IFFT operations and transmitted with CP via transmit antennas Tx1 and Tx2, respectively, as depicted in Figure 7. At the Rx, CPR is performed first. The two received signal vectors at time t and $t+T$ after FFT are

$$\boldsymbol{y}_1 = \boldsymbol{H}_1\boldsymbol{d}_1 + \boldsymbol{H}_2\boldsymbol{d}_2 \tag{10a}$$
$$\boldsymbol{y}_2 = -\boldsymbol{H}_1\boldsymbol{d}_2^* + \boldsymbol{H}_2\boldsymbol{d}_1^*. \tag{10b}$$

where $\boldsymbol{H}_1 \; and \; \boldsymbol{H}_2$ are two diagonal matrices whose diagonal elements are FFTs of respective channel impulse responses, $\boldsymbol{h}_1$ for the transmit antenna Tx1 and $\boldsymbol{h}_2$ for the transmit antenna Tx2. Assuming that fading is constant across two consecutive symbols in the rest of this paper, the decision variables are obtained as follows:

$$\hat{\boldsymbol{d}}_1 = \left(\boldsymbol{H}_1^*\boldsymbol{y}_1 + \boldsymbol{H}_2\boldsymbol{y}_2^*\right) = \left(\left|\boldsymbol{H}_1\right|^2 + \left|\boldsymbol{H}_2\right|^2\right)\boldsymbol{d}_1 \tag{11a}$$

$$\hat{\boldsymbol{d}}_2 = \left(\boldsymbol{H}_2^*\boldsymbol{y}_1 - \boldsymbol{H}_1\boldsymbol{y}_2^*\right) = \left(\left|\boldsymbol{H}_1\right|^2 + \left|\boldsymbol{H}_2\right|^2\right)\boldsymbol{d}_2 \tag{11b}$$

The STPC-OFDM Scheme

Since both the ST-OFDM and PC are techniques in a per- OFDM symbol basis, they can be integrated naturally. Figure 8 depicts a simplified block diagram of the STPC-OFDM transceiver. At the Tx, two length N consecutive blocks are formed as input data vectors at the Tx.

Similar to ST-OFDM, at time t, and $t+T$, $\boldsymbol{d}_1$ and $\boldsymbol{d}_2$, and $-\boldsymbol{d}_2^*$ and $\boldsymbol{d}_1^*$, are sent to two parallel branches for IFFT (upper branch) and FFT (lower branch) operations and transmitted with CP via transmit antennas Tx1 and Tx2, respectively, as depicted in Figure 8. Note that for simplicity, TDM is not shown explicitly at the Tx). At the Rx baseband, the upper branch employs a FFT for demodulating the received signal from Tx1 while the lower branch employs an IFFT for demodulating the received signal from Tx2. Note that the Rx needs to perform operations, for example, the de-multiplexing (DeMUX) operation (if TDM is employed at the Tx) to separate these two-branch signals. The received two signal vectors after FFT and IFFT at time t are

$$\boldsymbol{y}_{11} = FFT\left(\boldsymbol{h}_1 * IFFT(\boldsymbol{d}_1)\right) = \boldsymbol{H}_1\boldsymbol{d}_1 \tag{12a}$$

Figure 7. Block diagram of the regular ST-OFDM transceiver
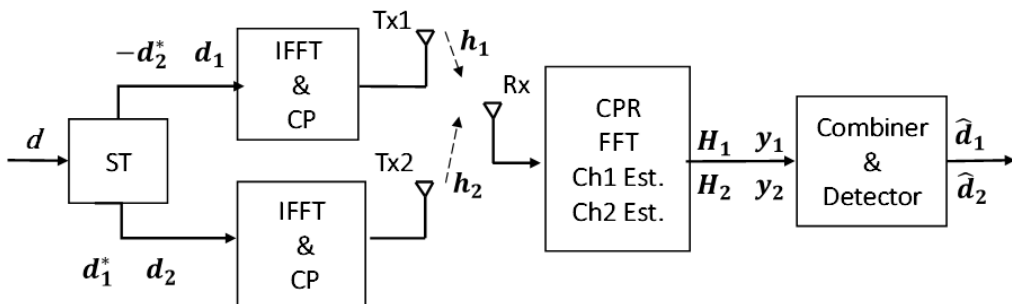
Figure 8. Block diagram of the STPC-OFDM transceiver
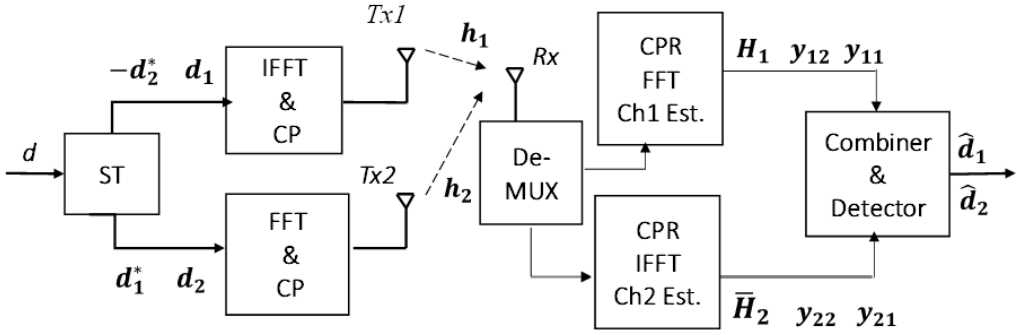
$$y_{21} = IFFT\left(h_2 * FFT(d_2)\right) = \bar{H}_2 d_2 \tag{12b}$$

where $\bar{H}_2$ is a diagonal matrix, whose diagonal elements are the N-point IFFTs of the channel impulse response h_2, and $*$ denotes the convolution operation. The first and second subindices ij of y_{ij} denote the Tx antenna and the time index, correspondingly. Similarly, the received two signal vectors after FFT and IFFT at time $t+T$ are

$$y_{12} = FFT\left(h_1 * IFFT\left(-d_2^*\right)\right) = -H_1 d_2^* \tag{13a}$$

$$y_{22} = IFFT\left(h_2 * FFT(d_1^*)\right) = \bar{H}_2 d_1^* \tag{13b}$$

The decision variables are defined as follows:

$$\hat{d}_1 = (H_1^* y_{11} + \bar{H}_2 y_{22}^*) / \left(\left|H_1\right|^2 + \left|\bar{H}_2\right|^2\right)\Box \tag{14a}$$

$$\hat{d}_2 = \left(\bar{H}_2^* y_{21} - H_1 y_{12}^*\right) / \left(\left|H_{11}\right|^2 + \left|\bar{H}_{12}\right|^2\right)\Box \tag{14b}$$

THE SEQUENTIAL IMPLEMENTATION SCHEME

This [2x1] STPC scheme can be simplified and implemented in a sequential manner.

Receiver Simplification

For example, at the transmitter, the antenna Tx1 transmits d_1 while the antenna Tx2 transmits 0. Successively, the antenna Tx1 transmits 0 while the antenna Tx2 sends d_1^*. Likewise, d_2 is also transmitted in a similar way. The receiver is then simplified and implemented in a TDM mode with FFT operation at time t, and IFFT operation at time $t+T$. This is a special case of the Alamouti scheme [6-7]. Obviously, it pays 50% in rate reduction because it uses only one antenna in transmission at any time instant.

Transmitter Simplification

Furthermore, the PC scheme can be implemented as a [1x1] system in a TDM mode. Only one branch is needed with a single transmitter and a single receiver. In other words, at the transmitter, the IFFT is

employed at time *t* and FFT is employed at time *t+T*. At the receiver, FFT is employed at time *t*, and IFFT is employed at time *t+T,* accordingly. Note that the IFFT operation can be performed by using the FFT processor (i.e., swapping the real and imaginary parts of the input sequence and swapping the real and imaginary parts of the output sequence).

In summary, the total computational requirement of the STPC scheme is the same as that of the ST scheme without increasing complexity, regardless of whether it is a two-branch or sequential one-branch implementation.

SIMULATION RESULTS

The performance of the PC and STPC schemes has been assessed by simulations. The COST207 channel parameters in Patzold (2012) are used for 4-ray rural (RA), and 6-ray typical urban (TU) and bad urban (BU) areas. These slow (RA) and fast (BU) frequency selective mobile channel parameters are applied to all simulations at a symbol rate of 2^{20} symbols/second and a sampling period of $Ts = 2^{-20}$ sec. A quarter of *N* samples is employed as the cyclic prefix.

Case 1: PC Scheme With Unknown Channels

The frequency domain differential coding is employed in order to avoid channel response estimation in three OFDM systems, DBPSK-regular, DQPSK-PC and DQPSK-SC. The bandwidth efficiency is 1 bit/Hz/s for all three systems. The transmitted power of the SC and each branch of the PC scheme is half of that of the regular DBPSK in order to have the same signal-to-noise ratio (SNR) as the DBPSK system. The maximum Doppler spread, f_D, to subcarrier frequency spacing ratio (i.e**.,** $\varepsilon_D = f_D N T_s$ is chosen as 0.01 and 0.2 in TU channel parameters with *N* = 8192. As depicted in Figure 9, when ε_D is large (i.e. 0.2), the BER of the SC scheme is better than that of the PC scheme, and the BER of the PC scheme is better than that of a regular DBPSK system. However, when ε_D is small (i.e., 0.01), the BER of the PC scheme outperforms that of the SC and DBPSK schemes, while the BER of the SC scheme is about the same as that of the DBPSK scheme. This shows a good agreement with the analytic results indicated in Section III. At a higher SNR, the BER curve of the PC scheme starts to exhibit an error floor due to ICI. Hence, the BER curve of the PC system becomes flat when *Eb/No* > 28 dB.

Case 2: STPC With Known Channels at the Receiver

Both the ST and STPC schemes employing QPSK modulation are studied. It is assumed that the channel responses, h_1 and h_2, are estimated and remain constant for *two* block periods.

Fig. 9 shows the average BER comparison with *N* = 512 and the maximum Doppler frequency range from 20 to 100 Hz (i.e., $\varepsilon_D = 0.01\,to\,0.05$ in the TU area. The STPC scheme outperforms the related ST scheme significantly in all cases due to the ICI cancellation. Note that the BER performance of these two systems in other areas is similar to that in the TU area. Hence, it is omitted here.

The error floor of the STPC scheme is always smaller than that of the ST scheme. Hence, the STPC scheme is robust for the OFDM block size and Doppler spread when the mobile multipath channel effects become the dominate factor at high SNR as depicted in Figure 10.

CONCLUSION

This tutorial paper comprehensively introduces the PC scheme for combating the impact of ICI in OFDM systems. The PC scheme, which has been studied theoretically and by simulations, provides a significant SICIR improvement over the SC scheme in small ε. Furthermore, we expand this PC scheme into a ST system and form a simple STPC scheme. By keeping useful properties of both the

Figure 9. BER comparison of regular-DBPSK, SC- DQPSK, and PC-DQPSK systems in TU channels
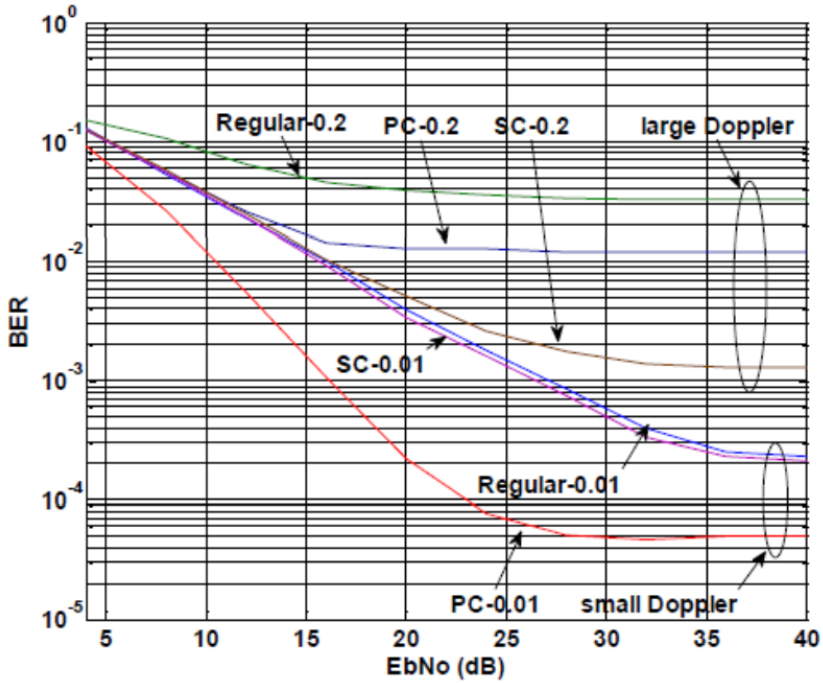
Figure 10. Average BER comparison of the STPC-QPSK and ST-QPSK schemes with the OFDM block size N=512 and the maximum Doppler frequency range from 20 Hz to 100 Hz in TU area
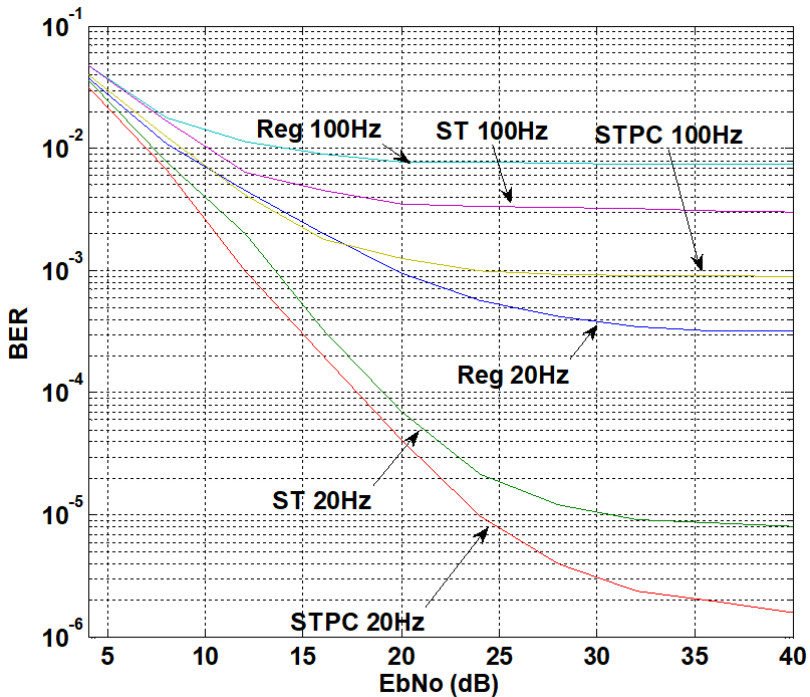
ST (robust to OFDM symbol size) and PC (ICI cancellation) schemes, the STPC outperforms regular ST-OFDM and PC-OFDM systems in mobile channels without increasing system complexity. This STPC-OFDM has a significantly lower error floor due to the ICI parallel cancelling scheme in both slow and fast frequency selective fading channels. Although only a [2x1] transmitter diversity scheme is presented, it can be applied to other MIMO systems, such as a [2x2] system, and MISO and MIMO, such as a [4x1]. Since this STPC is very simple, it may serve as the enhanced function with almost no additional cost in hardware and software when it is combined with other channel coding scheme to mitigate ICI and improve BER performance in mobile channels with residual frequency offset, timing offset, or Doppler velocity.

REFERENCES

Alamouti, S. M. (1988). A simple transmit diversity technique for wireless communications. *IEEE Journal on Selected Areas in Communications*, *16*(8), 1451–1458. doi:10.1109/49.730453

Chang, D. C. D. (2012). Dynamic Power Allocation via Wavefront Multiplexing Through Multiple Base Stations. *IEEE Global Communications Conference*, 3813-3818. doi:10.1109/GLOCOM.2012.6503707

Chang, D. C. D. (2013a). Orthogonal wavefront multiplexing architecture for communications in non-contiguous channels. *Wireless Telecommunications Symposium*, 1-10. doi:10.1109/WTS.2013.6566242

Chang, D. C. D. (2013b). Coherent Power Combining on Spacecraft via Wavefront Multiplexing Techniques. *IEEE International Conference on Computing, Networking and Communications Workshop*, 268-272. doi:10.1109/ICCNC.2013.6504093

Kumar, P. V., & Rao, N. V. (2018). A novel method for ICI cancellation in OFDM system. *International Conference on Electrical, Electronics, Communication, Computer Technologies and Optimization Techniques)*, 1036-1041. doi:10.1109/ICEECCOT43722.2018.9001368

Li, Z., & Xia, X.-G. (2008). An Alamouti Coded OFDM Transmission for Cooperative Systems Robust to Both Timing Errors and Frequency offsets. *IEEE Transactions on Wireless Communications*, *7*(5), 1839–1844. doi:10.1109/TWC.2008.070443

Ma, T.-M. (2017). A novel PRCC scheme for OFDM systems over frequency-selective fading channels. *IEEE Signal Processing Letters*, *24*(5), 634–637. doi:10.1109/LSP.2017.2686899

Nasir, A. A., Durrani, S., Mehrpouyan, H., Blostein, S. D., & Kennedy, R. A. (2016). Timing and carrier synchronization in wireless communication systems: A survey and classification of research in the last 5 years. *EURASIP Journal on Wireless Communications and Networking*, *180*(1), 180. Advance online publication. doi:10.1186/s13638-016-0670-9

Patzold, M. (2012). Mobile Radio Channels. Wiley.

Seyedi, A., & Saulnier, G. J. (2005). General ICI Self-Cancellation scheme for OFDM systems. *IEEE Transactions on Vehicular Technology*, *54*(1), 198–210. doi:10.1109/TVT.2004.838849

Wen, M. (2013a). Two-path transmission framework for ICI reduction in OFDM systems. *IEEE Global Communications Conference*, 1-6.

Wen, M. (2013b). Effective intercarrier interference reduction techniques for OFDM underwater acoustic communications. *Signals Systems and Computers Asilomar Conference*, 93-97. doi:10.1109/ACSSC.2013.6810237

Yeh, H. G., Chang, Y. K., & Hassibi, B. (2007). A scheme for canceling intercarrier interference through conjugate transmission for multicarrier communication systems. *IEEE Transactions on Wireless Communications*, *6*(1), 3–7. doi:10.1109/TWC.2007.04541

Yeh, H.-G., & Ingerson, P. (2010). Software-Defined Radio for OFDM Transceivers. *IEEE International Systems Conference,* 1-6/

Yeh, H. G., & Wang, C. C. (2004). New parallel algorithm for mitigating the frequency offset of OFDM systems. *IEEE Vehicular Technology Conference*, 2087-2091.

Yeh, H. G., & Zhou, J. (2022a). BER Performance of Pre-coded Space-Time Conjugate Two-Path OFDM Systems. *International Journal of Interdisciplinary Telecommunications and Networking*, *14*(1), 1–13. doi:10.4018/IJITN.299364

Yeh, H. G., & Zhou, J. (2022b). Design Switchable Precoded Space-Time Parallel Two-Path OFDM Systems. *International Journal of Interdisciplinary Telecommunications and Networking*, *14*(1), 1–12. doi:10.4018/IJITN.299367

Yu, Y., Leung, S.-H., & Lu, F. (2007). Iterative frequency domain equalization for OFDM over doubly selective channels. *IEEE International Conference on Acoustics, Speech, and Signal Processing*, 3, 453-456. doi:10.1109/ICASSP.2007.366570

Yusof, S. K. S., & Zamani, A. I. A. (2008). Intercarrier Interference Self-Cancellation for Space-Time-Frequency MIMO-OFDM System. *IEEE International RF and Microwave Conf.*, 520-523. doi:10.1109/RFM.2008.4897452

Zhao, Y., & Haggman, S.-G. (2001). Intercarrier interference self-cancellation scheme for OFDM mobile communication systems. *IEEE Transactions on Communications*, *49*(7), 1185–1191. doi:10.1109/26.935159

Hen-Geul Yeh (SM'82) received the B.S. degree in engineering science from National Chen Kung University, Taiwan, ROC, in 1978, and the M.S. degree in mechanical engineering and the Ph.D. degree in electrical engineering from the University of California, Irvine, in 1979 and 1982, respectively. Since 1983, he has been with the Electrical Engineering department at California State University, Long Beach (CSULB), USA, and served as the department Chair since 2016. His research interests include DSP/Communication/Control/Smart Systems algorithms development and implementation with applications to communication, smart grids, optimization, controls, and electrical event detection with more than 150 research papers in these areas. Dr. Yeh is the recipient of IEEE R6 Outstanding Engineering Educator Award for outstanding contribution to the education of electrical engineers in the areas of DSP, Green Energy, and smart systems in 2019, Outstanding Professor Award, CSULB, 2015, five NASA Tech. Brief and New Technology awards from the National Aeronautics and Space Administration (NASA) from 1987 to 1996, and the Northrop Grumman Excellence in Teaching award, CSULB, 2007. Since 2010, he has served as the Founder and Chair of IEEE Green Energy and Smart Systems Conference (IGESSC).